

On the Disintegration Products of the 2.2- μ Sec. Meson

E. P. HINCKS AND B. PONTECORVO*

National Research Council of Canada, Chalk River Laboratory, Chalk River, Ontario, Canada

(Received September 19, 1949)

An investigation of the penetration through absorbers of various elements by the charged particles that result from the 2.2- μ sec. meson decay is reported. Mesons and decay particles are detected by an arrangement of Geiger-Müller counter trays, and delayed coincidence techniques are used to select the desired events. The absorption measurements exhibit two components in the decay radiation, one of which is much more penetrating than the other. In lead, for example, the "soft component" is essentially absorbed by about 20 g/cm², while the "hard component" is easily detected after 38 g/cm².

A different arrangement of counters is used to show that the "hard component" is due to a neutral radiation which accompanies the charged decay particles. This result, and measurements of the intensities of the "hard component" with lead and carbon

absorbers, provide strong evidence that the neutral radiation is, in fact, bremsstrahlung from the charged particles which constitute the "soft component."

The bremsstrahlung intensities, together with the form of the absorption curve, are shown to lead to the following conclusions: (1) the charged decay particles are electrons (i.e., they have a mass less than two electron masses); (2) a considerable number of electrons are emitted with energies greater than 25 Mev; (3) the average energy of the electrons is greater than 25 Mev; (4) there is no evidence for electrons of energy much greater than 50 Mev.

The support which these results lend to the currently favored ideas on the meson decay process is discussed.

INTRODUCTION

THE decay process of the ordinary cosmic-ray meson^a is still not known with certainty, although its instability was first inferred over ten years ago. The earliest direct observations of the decay phenomenon were made in a cloud-chamber photograph by Williams and Roberts¹ in 1940, and by the detection of the delayed emission of charged particles from stopped mesons by Rasetti,² and by Auger, Maze, and Chaminade,³ in 1941.

The photograph by Williams and Roberts (as well as others which have been obtained subsequently⁴), showed that a single lightly ionizing charged particle is emitted in the decay process. This observation provided evidence for the identity of the cosmic-ray meson and the particle postulated earlier by Yukawa to account for nuclear forces,⁵ and this identification was made even more convincing by the similarities between the lifetimes and between the masses of the two particles. The hypothetical Yukawa meson has integral spin,

* Present address: Atomic Energy Research Establishment, Harwell, England.

^a By "cosmic-ray meson" we mean the particle, positive or negative, of mass about 100 Mev, that forms the bulk of the hard component of the cosmic radiation at sea level and decays, when free, with a mean life of 2.2 μ sec. It is commonly assumed to be identical with the μ -meson produced in the π - μ -decay process discovered by Lattes, Occhialini, and Powell (Nature **160**, 453 (1947)). In this paper the term meson will refer to the 2.2- μ sec. particle unless otherwise specified.

¹ E. J. Williams and G. E. Roberts, Nature **145**, 102 (1940).

² F. Rasetti, Phys. Rev. **59**, 613 (1941); **60**, 198 (1941).

³ Auger, Maze, and Chaminade, Comptes Rendus **213**, 381 (1941).

⁴ Fowler, Cool and Street, Phys. Rev. **74**, 101 (1948); R. W. Thompson, Phys. Rev. **74**, 490 (1948); Kan-Chang Wang and S. B. Jones, Phys. Rev. **74**, 1547 (1948). It should be noted that Thompson's cloud chamber was triggered by delayed coincidences, and therefore the correlation was almost certainly established between the events observed and the 2.2- μ sec. decay. (See also references 11 and 18).

⁵ For a discussion and references see, for example, *Cosmic Radiation*, edited by W. Heisenberg (Dover Publications, New York, 1946).

and, when free, disappears in the following process:

$$\text{meson} \rightarrow \text{electron} + \text{neutrino}. \quad (1)$$

Conservation of energy and momentum requires both decay products to receive as kinetic energy about half the rest mass (~ 100 Mev) of the meson. According to the Yukawa picture, positive mesons when brought to rest should decay with the production of electrons (positive) of about 50 Mev; negative mesons, on the other hand, are expected⁶ to be captured by nuclei of the stopping material in a time much shorter than their lifetime for radioactive decay, and so give rise to no decay radiation. The energy— 70 ± 35 Mev—of the decay particle in Williams and Roberts' picture was consistent with the assumption of Eq. (1). Moreover, Conversi and Piccioni⁷ in 1944 deduced from the numbers of decay particles escaping from iron plates 0.6 cm and 5 cm thick that their mean range is about 2.5 cm of iron. This value corresponds to an electron energy of about 50 Mev, again in agreement with the electron-neutrino hypothesis.

A refutation of the identification of the 2.2- μ sec. meson with the Yukawa particle was given by the well-known experiment of Conversi, Pancini and Piccioni,⁸ which showed that while in a heavy element (iron) only *positive* stopped mesons decay, in a light element (carbon), on the other hand, both *positive and negative* mesons decay. This result and subsequent confirmative experiments by other workers lead to the conclusion^{8,9} that the interaction between the meson

⁶ S. Tomonaga and G. Araki, Phys. Rev. **58**, 90 (1940).

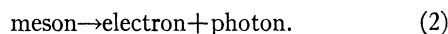
⁷ M. Conversi and O. Piccioni, Phys. Rev. **70**, 874 (1946).

⁸ Conversi, Pancini, and Piccioni, Phys. Rev. **71**, 209 (1947).

⁹ J. A. Wheeler, Phys. Rev. **71**, 320 (1947); E. Fermi, E. Teller and V. Weisskopf, Phys. Rev. **71**, 314 (1947); E. Fermi and E. Teller, Phys. Rev. **72**, 399 (1947); T. Sigurgeirsson and A. Yamakawa, Phys. Rev. **71**, 319 (1947); G. E. Valley, Phys. Rev. **72**, 772 (1947); H. K. Ticho and M. Schein, Phys. Rev. **73**, 81 (1948); G. E. Valley and B. Rossi, Phys. Rev. **73**, 177 (1948);

and the nucleus is much smaller (by a factor $\sim 10^{12}$) than that required for the Yukawa particle, and so precludes the possibility of their identity. In renouncing the "Yukawa character" of the meson, we must also renounce the inferences regarding its decay products and its spin. In particular, we must admit that not only may the neutrino of Eq. (1) be replaced by some other neutral particle, or particles, but also that *the charged decay particle may not be an electron.*

Another decay process which would result in electrons of about 50 Mev, but which would require half-integral spin for the meson, is the following:



This process is, however, apparently ruled out by the negative results of several workers¹⁰ who searched for photons from disintegrating mesons.

The observation of a meson disintegration in a cloud chamber, in which the energy of the decay particle is 24 Mev, led Anderson and co-workers¹¹ to suggest the process:



the mass of the neutretto, or neutral meson, being 25–30 Mev less than that of the original meson. While the secondary charged particle was assumed to be an electron, by direct measurements of momentum and specific ionization these authors could only place an upper limit to its mass at about 25 electron masses.

The experiments^b to be described in this paper were undertaken in order to derive some information about the nature and energy of the charged decay particles by observing their penetration through solid matter. The measurements were made at the Chalk River Laboratory, near sea level, in the period May, November, 1948. Since the present work was initiated, new results^{4,12,13} relating to the energy spectrum of the charged particles have appeared in the literature. Steinberger,¹³ in particular, has made absorption measurements similar in principle to our own, and we shall discuss them further below.

C. W. Kissinger and D. Cooper, Phys. Rev. **74**, 349 (1948); H. K. Ticho, Phys. Rev. **74**, 492 (1948); **74**, 1337 (1948).

¹⁰ R. D. Sard and E. J. Althaus, Phys. Rev. **73**, 1251 (1948); **74**, 1364 (1948); E. P. Hincks and B. Pontecorvo, Phys. Rev. **73**, 257 (1948); a full report has been submitted for publication in Can. J. Research; O. Piccioni, Phys. Rev. **74**, 1236 (1948); **74**, 1754 (1948).

¹¹ Anderson, Adams, Lloyd, and Rau, Phys. Rev. **72**, 724 (1947). A second photograph, in which the decay particle energy is 25 Mev, was published by Adams, Anderson, Lloyd, Rau, and Saxena, Rev. Mod. Phys. **20**, 334 (1948).

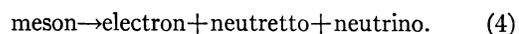
^b Partial accounts of the results of these experiments have been presented at the Royal Society of Canada, Vancouver Meeting, June 1948, and at the American Physical Society, Chicago Meeting, November 1948; also in Phys. Rev. **74**, 697 (1948); **75**, 698 (1949).

¹² J. G. Retallack, Phys. Rev. **73**, 921 (1948); Zar, Herschkowitz, and Berezin, Phys. Rev. **74**, 111 (1948); M. H. Shamos and A. Russek, Phys. Rev. **74**, 1545 (1948).

¹³ J. Steinberger, Phys. Rev. **74**, 500 (1948); **75**, 1136 (1949). We are indebted to Dr. Steinberger for sending us a complete account of his work in advance of publication.

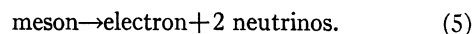
While the form of the energy spectrum of the decay particles still requires further investigation, it seems certain, at least, that it does not consist of a single line. The possible alternatives are several lines (i.e., two or more competing decay processes), or a continuum, (i.e., three or more decay products).

As an example of a process with three decay products, the following has been suggested:¹⁴



This process would result in a continuous spectrum of electron energies with a maximum energy equal to less than half the mass of the original meson by an amount dependent upon the mass of the neutretto, and with an average energy somewhat greater than half the maximum. Equation (4) like Eq. (3) requires the existence of a new particle, the neutretto or neutral meson, which might be expected on theoretical grounds to have a very short lifetime for decay into photons. There is some experimental evidence^{10,15} against this possibility.

Another process which would result in a continuous distribution of electron energies was mentioned by Nordheim¹⁶ in 1941:



Good evidence for a continuous spectrum of the decay particles was published recently by Brown *et al.*¹⁷ and by Leighton *et al.*,¹⁸ after our work as well as Steinberger's was finished. The California authors measured in a cloud chamber the momenta of a great number of decay charged particles, contributing most of the present knowledge on the energy spectrum. Their results support the process (5).

Part I of the present paper describes measurements pertinent to the problem of the energy of the decay charged particles. Part II concerns the nature (mass) of such particles. We shall discuss our results in relation to the several hypotheses mentioned above, and in particular, at the end of the paper, summarize the evidence supporting process (5).

PART I. ABSORPTION MEASUREMENTS

1. Method

The function of the apparatus used in this experiment is to select charged particles which result from the meson decay process and which have traversed a known thickness of matter. The numbers of such events may then be observed for absorbers of different thicknesses, and of different materials. Some of the more important considerations affecting the choice of a suitable experimental arrangement are worthy of mention.

¹⁴ O. Klein, Nature **161**, 897 (1948); Horowitz, Kofoed-Hansen, and Lindhard, Phys. Rev. **74**, 713 (1948).

¹⁵ E. P. Hincks and B. Pontecorvo, Phys. Rev. **73**, 1122 (1948).

¹⁶ L. W. Nordheim, Phys. Rev. **59**, 554 (1941).

¹⁷ Brown, Camerini, Fowler, Muirhead, Powell, and Ritson, Nature **163**, 47 (1949).

¹⁸ Leighton, Anderson, and Seriff, Phys. Rev. **75**, 1432 (1949).

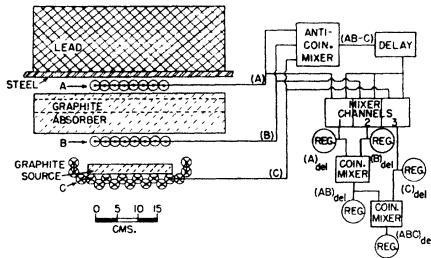


FIG. 1. Experimental arrangement for the absorption measurements, with block diagram indicating the essential functions of the electronic circuits. The geometry perpendicular to the paper may be inferred from the lengths of the source and counters, which are ~ 40 cm.

To detect both mesons and decay particles, the use of Geiger counters (in trays of many counters each) permits a relatively high rate of useful events to be obtained because large effective areas are possible, and the counters (at the counting rates used) are essentially continuously sensitive. The desired events, i.e., the stopping of mesons, followed by their decay with the emission of charged particles, are selected by the well-known technique of delayed coincidences. We have chosen for its directness and flexibility an arrangement in which the material which absorbs mesons, which we shall refer to as the "source" of decay particles, is separate from the material which absorbs the decay particles, to be called the "absorber."

The choice of source is governed by the requirement that decay particles should not lose too much energy in it before escaping. Therefore its thickness must be small compared with the average range of the decay particles. However, in order that the number of mesons stopped be not too low, a compromise must be made. The use of an element of low atomic number for the source has two advantages: (1) loss of energy by bremsstrahlung, with its resultant severe straggling, will be minimized; and (2) the intensity is enhanced by the decay of negative, as well as positive mesons. The source used was carbon, and its thickness— 4.2 g/cm^2 —is about one-third the average range of 25-Mev electrons.

The requirement of a counting rate high enough to permit absorption measurements to be made in a reasonable time not only limits the thinness of the source, but also restricts the amount of collimation which can be imposed on the decay particles in their passage through the absorber. Thus we expect¹⁹ about 0.03 meson stopped per gram of source per hour, or a total in our source (mass 3300 grams) of about 100 mesons stopped per hour. The condition that the meson should traverse a counter telescope renders only a fraction ($\sim 1/3$ in our geometry) of these useful as a source of decay particles. Clearly then, "good geometry" for the absorption measurements must be sacrificed for intensity.

¹⁹ Data may be obtained from B. Rossi, Rev. Mod. Phys. 20, 537 (1948).

Absorbers of carbon, aluminum, and lead were used. Again a low Z material (preferably the same as the source), i.e., carbon, will facilitate interpretation of the results because of smaller bremsstrahlung effects. On the other hand, because of its low density, large thicknesses of such a material cannot be used without expanding the apparatus, and therefore losing intensity. Aluminum is a compromise in this respect, while lead was used to obtain a comparison between absorbers of high and low Z . The areas of all absorbers were such that they extended on all sides well beyond the solid angle defined by the counters.

2. Arrangement of Apparatus

In Fig. 1 we show a vertical section of the arrangement of counters and absorbers together with a simplified block diagram of the counting circuits. The apparatus was situated in a room whose walls and ceiling were concrete. Figure 2 is a photograph of the counter assembly; the components may be easily identified by comparison with the left-hand side of Fig. 1.

Three trays of counters are used, from top to bottom, A , B , and C (Fig. 1). Trays A and B each consist of 8 counters, each 1-in. diameter and 15-in. active length, with 1-mm thick copper walls. They are supported in thin aluminum boxes, but the bottom of box A , and the top and bottom of box B , are cut away to expose the active areas of the counters. The 17 counters of tray C are 1-in. diameter, 16-in. active length, with 0.65-mm thick brass walls, and are supported on a thin (0.5 g/cm^2) aluminum shelf about 4 ft. above the floor of the room. All counters used were of the self-quenching type. A graphite block ($20 \text{ cm} \times 40 \text{ cm} \times 4.2 \text{ g/cm}^2$ thick; density=1.7) resting on the counters of tray C forms the source of decay particles. Mesons traversing trays A and B , and stopping in the source, are detected by the anticoincidence ($AB-C$). The pulse corresponding to ($AB-C$), which we shall refer to as the "triggering event," is first delayed $\sim 1 \mu\text{sec.}$ and then initiates a gating pulse $\sim 5 \mu\text{sec.}$ wide. The outputs of each of trays A , B , and C are separately mixed with the gating pulse in such a way that if a discharge of either A , B , or C occurs between 1 and $6 \mu\text{sec.}$ after a triggering event, a "delayed coincidence" is recorded which we designate as (A)_{del}, (B)_{del}, or (C)_{del} respectively. A decay particle leaving the source between 1 and $6 \mu\text{sec.}$ after a meson stops will thus be detected in any of the three trays through which it passes. In particular, a decay particle passing upward through both B and A gives a delayed coincidence (AB)_{del}.

The absorbers are placed in the 10-cm gap between trays A and B . They consist of aluminum sheets, lead sheets, or graphite blocks (density=1.7), and in all cases cover an area about 50 cm square. While the graphite and aluminum absorbers always rested on the top of the B counter box, the lead absorbers (with the exception of the very thick ones), were supported about

midway between trays *A* and *B*. When it turned out to be of interest to use graphite absorbers with a thickness greater than 10 cm, a compromise was made by adding a thickness of heavier material—iron or copper—above an initial thickness of graphite.

The lead (15 cm thick = 170 g/cm²) which is placed above *A* (together with the concrete ceiling of the room), serves not only to shield the counters from the soft cosmic-ray component, but also, because of the form of the differential range spectrum of mesons,¹⁹ to increase somewhat the “source strength,” i.e., the number of mesons stopped in the source. On the other hand we expect that the source strength will not be altered significantly by the addition of the absorbers (up to ~ 100 g/cm²) between *A* and *B*, an assumption which was verified experimentally by control measurements made during the experiment.

The geometry used, in which decay particles emitted *upward* from the source are detected by the same pair of counter trays that detect the incident mesons, was chosen for its considerable economy in counters for a given intensity. However, although trays *A* and *B* are each used for two purposes, two properties of this geometry which reduce the efficiency should be noted: (1) the collimation of the meson beam, similar to that of the decay particles, is unnecessarily high, and (2) at least one counter in both *A* and *B*—the one discharged by the meson—is insensitive to a decay particle which may traverse it. The decrease in sensitivity of tray *B* due to the dead counter would be serious if the source were too close, and a favorable position of the latter (4.1 cm below *B*) was determined graphically.

The dual use of trays *A* and *B* introduces some complication in the electronic circuits, which will be described in the next section. On the other hand the arrangement lends itself to the reduction of the background (casual) counting rate by means of the anticoincidence counters *C*. The anticoincidence function of tray *C* for the *triggering event* (*AB*–*C*) has already been stated. Moreover, since essentially all the casual *delayed events* are caused by a second meson traversing the apparatus by chance within the delayed resolving time, by recording (*ABC*)_{del} together with (*AB*)_{del} we can identify a large fraction of these events and disregard them. In effect, therefore, we measure the counting rate

$$(AB-C)_{\text{del}} = (AB)_{\text{del}} - (ABC)_{\text{del}}$$

with various absorbers between trays *A* and *B*. While the anticoincidence efficiency of tray *C* in our arrangement is not very high (of the mesons which traverse *A* and *B*, far more “leak” past *C* than stop in the source), nevertheless it is sufficient to give a very low rate of casual (*AB*–*C*)_{del} events.

3. Electronic Apparatus

Figure 3 is a complete block diagram showing the electronic components used to record the delayed events.

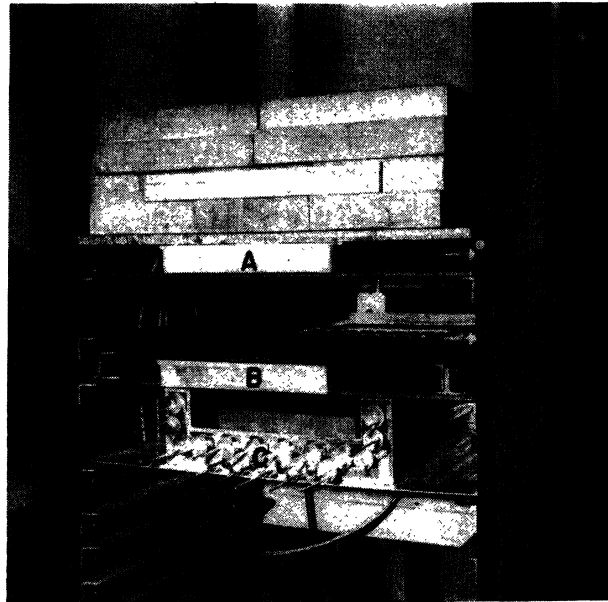


FIG. 2. Photograph of the counter assembly showing the graphite source between trays *B* and *C*. Absorbers are placed in the space between trays *A* and *B*.

Each counter used has a separate H.T. resistor ($R = 10^7$ ohms) by which voltage is applied to the wire, and a separate output condenser ($C = 50 \mu\text{mf}$). In tray *C* the counters are simply paralleled by connecting all 17 output condensers to the input of a single cathode-follower. On the other hand the circuits associated with trays *A* and *B* must be capable of handling two pulses which may be as close together as 1 $\mu\text{sec.}$ and, moreover, the first pulse of the pair must be accepted by the anticoincidence mixer, while the second must be accepted by the delay mixer. It will be apparent that to satisfy the last requirement it must be ensured that *either* there be no dead-times equal to or greater than one microsecond between the output of the counter tray and the mixing stage of the delay mixer, *or* if there be a long dead-time at some stage, then the first pulse must be prevented from reaching it and rendering it insensitive to the second pulse. The second of these conditions has been satisfied in our apparatus. The delay mixer input circuit has a long dead-time ($\sim 100 \mu\text{sec.}$) but when operated from the “threshold amplifier” (“threshold output”) it receives only the *second* of two pulses which occur close together. From the “normal output” of the threshold amplifier, on the other hand, the first pulse of the pair is fed to the anticoincidence mixer.

A circuit diagram of the threshold amplifier* is shown

* The characteristics of the “threshold amplifier” make it of possible use for several purposes. It may have application, for example, as a coincidence (or anticoincidence) mixer in counter arrays in which the functions of the counters are not individually specified. Thus by selecting output pulses of the appropriate magnitude, events in which only one, or only two, or two or

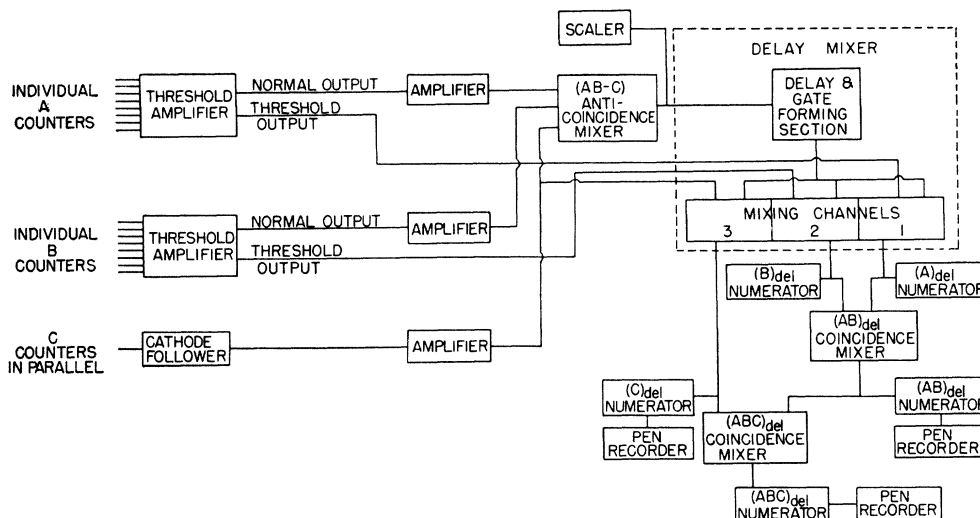


Fig. 3. Detailed block diagram of the circuits used to record the delayed coincidences in the absorption measurements.

in Fig. 4. The output of each counter of the tray is fed to a separate tube (6AU6) whose purpose is to shape and equalize all pulses. Thus, the negative pulse resulting from a counter discharge cuts off the plate current of the associated 6AU6 very quickly (in $\sim 0.1 \mu\text{sec.}$) with the result that at the plate an approximately rectangular positive pulse appears whose width (10–15 $\mu\text{sec.}$) is determined by the differentiating time constant at the grid. The amplitude of this pulse is given by the steady potential drop across the 10K plate resistor of the tube, and standardization of the pulse sizes from different tubes is improved by using both matched tubes and matched plate resistors. The outputs of all tubes are mixed in a resistor network and output stage (6AQ5) whose operation is linear over the region in which it is used. (The use of negative feedback from plate to grid has the advantages of improving the linearity, and of reducing the output impedance.) Thus the discharge of a single counter results in a rectangular negative pulse at the 6AQ5 plate; the simultaneous discharge of two counters produces a rectangular pulse of twice the amplitude, and so on. A diode discriminator (EA50), with its bias adjusted to a voltage just greater than the amplitude of a single pulse, will therefore pass a standard pulse which has been preceded within an interval 0 to $\sim 15 \mu\text{sec.}$ by another standard pulse. In our application of this circuit, the discharge of one counter by a meson initiates a pulse which reaches the anticoincidence mixer via the “normal output” (no discriminator). On the other hand, only a second pulse, e.g., that due to a decay particle with a delay between 0 and 15 $\mu\text{sec.}$, can pass the “threshold output” to

more, etc., counters are discharged may be selected. While the present circuit has been designed for maximum simplicity, some refinements in the pulse shaping stages would give greater uniformity of size, and would be required for coincidences of higher order.

trigger the input circuit of the delay mixer. All components of the circuit (excluding power supply) are mounted directly on the end of the counter box. It is essential that the leads from the counters to the 6AU6 grids be short, and shielded from each other, but the output impedance is sufficiently low to tolerate several feet of low capacity cable.

The “normal outputs” of the threshold amplifiers of trays *A* and *B* feed the two “coincidence inputs” of the anticoincidence mixer through “wave-front amplifiers.” The latter are simply fast two-stage saturating amplifiers (gain below saturation $\sim 10^3$) which serve to bring the pulse front above the threshold of the anticoincidence mixer with negligible delay. In the case of tray *C*, where no threshold amplifier is required, the pulses are fed from a cathode-follower through a wave-front amplifier, and thence to the “anticoincidence input” of the mixer.

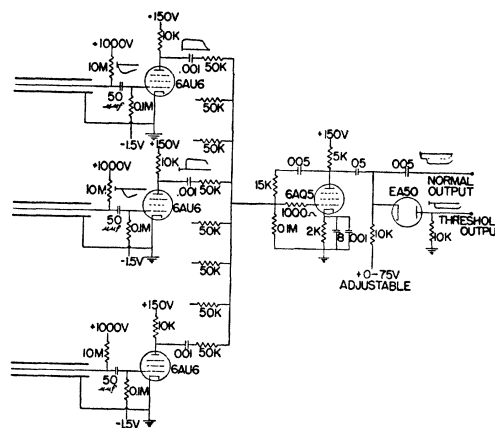


Fig. 4. Schematic diagram of the threshold amplifier circuit, showing three of the eight parallel input stages with G-M counters.

TABLE I. Summary of $(AB-C)_{\text{del}}$ rates for "no absorber" runs.

Two-week period	Hours of observation	$(AB-C)_{\text{del}}$ Total counts	$(AB)_{\text{del}} - (ABC)_{\text{del}}$ Counts/hr.*
May 1-15	99	89	0.90 ± 0.10
June 1-15	71	50	0.70 ± 0.10
June 16-30	50	34	0.68 ± 0.12
July 1-15	30	22	0.73 ± 0.16
Aug. 1-15	49	39	0.80 ± 0.13
Aug. 16-31	87	65	0.75 ± 0.09
Sept. 1-15	22	16	0.73 ± 0.18
Total	408	315	0.77 ± 0.05

* All errors ascribed to measured counting rates in this paper are the statistical standard deviations.

one of the delay channels, the mixing tube (6AS6), which is normally cut off, receives positive standard pulses from the thyratron cathode of that channel on its suppressor grid, and positive gating pulses on its control grid. When these are coincident (the total resolving time is slightly less than the sum of the two pulse widths), a negative pulse appears at the mixer plate and drives the output tube ($\frac{1}{2}$ -2C51). From the cathode of the latter negative pulses are available for external use; from the plate positive pulses operate a built-in numerator (mechanical register operated by a thyratron). The delayed coincidences in the three channels are thus counted independently by three numerators; a fourth (spare) numerator, with a separate external input, is a useful addition. Each numerator has an output terminal whence a pulse may be obtained to drive the pen of a chart recorder so that, if desirable, the time of occurrence of a delayed coincidence may be observed.

The triggering input of the delay mixer is fed by the output of the anticoincidence mixer. The rate of triggering events $(AB-C)$ in the delay mixer is continuously monitored by a scaler. Delay channels 1, 2, 3, are fed by the "threshold output" from tray *A*, the "threshold output" from tray *B*, and the wave-front amplifier output from tray *C*, respectively; the outputs of these channels therefore correspond to the events $(A)_{\text{del}}$, $(B)_{\text{del}}$ and $(C)_{\text{del}}$. The events $(AB)_{\text{del}}$ are detected by mixing the $(A)_{\text{del}}$ and $(B)_{\text{del}}$ outputs in a two-channel coincidence mixer (resolving time = 0.6 μ sec.) and the events $(ABC)_{\text{del}}$ are detected by mixing the output of the $(AB)_{\text{del}}$ mixer with the $(C)_{\text{del}}$ output in a second two-channel mixer (resolving time = 8 μ sec.). All delayed events are counted by individual numerators (it is arranged as a check that each delayed event is counted by two numerators fed from different points of the circuit), and the events $(AB)_{\text{del}}$, $(ABC)_{\text{del}}$ and $(C)_{\text{del}}$ are recorded on the moving charts of synchronized Esterline Angus recording milliammeters. The circuits of the two-channel coincidence mixers are similar to that given by Jelley,²⁰ while the individual numerators each consist of a mechanical register and driving circuit, as used in the delay mixer.

The a.c. power is supplied to the electronic apparatus, with the exception of a few units whose operation is

not critical, through voltage-regulating transformers. The d.c. voltages required for the counters are obtained from compact 1200-v battery boxes with stepped outputs. A separate battery supplies the single operating voltage for each tray of counters.

4. Control Measurements

Many control runs, and tests of the proper operation of the apparatus, were made during the many months taken by the experiment. These checks may be divided into three categories: (a) those obtained continuously during the experimental runs, (b) those made periodically, once or twice a day, and (c) those made only occasionally. They will be described in turn.

(a) *Continuous checks.*—(i) The number of triggering events $(AB-C)$ was counted continuously by a scaler. Readings taken usually twice a day showed whether the $(AB-C)$ rate had been normal throughout the preceding interval. The rate varied somewhat (between 30/min. and 37/min.), as expected, when different absorbers were inserted between trays *A* and *B*, but for a given condition fluctuations from the mean value were never more than a few percent, and often much less, over long periods.

(ii) The rates $(B)_{\text{del}}$ and $(C)_{\text{del}}$, and therefore their sum $(B)_{\text{del}} + (C)_{\text{del}}$, are due chiefly to decay electrons from the source and so constitute an excellent check (a) of the constancy of the "source strength," (b) of the constancy of the delay and gate width of the delay mixer, and (c) of the proper performance of the *B*- and *C*-tray counters and their associated circuits. Twice-daily readings furnished interim checks, while the rates averaged over the complete run with a given absorber furnished a suitable reference intensity for that run. Fluctuations in these averaged rates with different absorbers were not appreciably greater than those expected from statistical causes, and, since the statistical errors in the $(AB-C)_{\text{del}}$ rates were at all times much greater, corrections for variation in "source strength" could be neglected. The mean $(B)_{\text{del}}$ rate during the whole experiment (2155 hours of observation) was 4.1/hr.; the mean $(C)_{\text{del}}$ rate was 8.6/hr.

(iii) The Esterline-Angus charts were examined carefully for evidence of non-randomness in the rates $(AB)_{\text{del}}$, $(ABC)_{\text{del}}$, or $(C)_{\text{del}}$, for assurance that each $(ABC)_{\text{del}}$ count was properly coincident with an $(AB)_{\text{del}}$ count, and for evidence of power failure or other irregularity.

(b) *Periodic Checks.*—(i) Measurements of the single counting rates (A) , (B) , (C) (i.e., the total rate of each tray separately), indicated that the sensitivity of each tray was normal. The single rates varied somewhat with changes in absorber, and, of course, with drifts in the H.T. voltages, but the good reproducibility attained with a given absorber may be attributed in large part to the excellent characteristics of the counters. Typical values of the single rates with a thick absorber (80

g/cm² Pb) are:

$$\begin{aligned}(A) &= 720/\text{min.} \\ (B) &= 1030/\text{min.} \\ (C) &= 2690/\text{min.}\end{aligned}$$

(ii) The H.T. voltages supplied by the batteries to each tray of counters were checked, and readjusted when a drift $\sim \pm 10$ v occurred.

(iii) Some of the more critical d.c. voltages in the coincidence mixers were checked, and readjusted if they drifted beyond safe limits.

(iv) The shapes of certain standard pulses produced in the delay mixer were observed with a fast oscilloscope.

(c) *Occasional Checks.*—(i) Control runs were made at appropriate intervals throughout the experiment with no decay particle absorber. In these “no absorber” runs the rate $(AB-C)_{\text{del}}$ checks the sensitivity and proper performance of the whole apparatus. That this rate did not exhibit significant variation may be seen from Table I, in which the values are grouped according to the two-week period during which they were obtained. The mean rate ($0.77 \pm 0.05/\text{hr.}$) has been taken as a measure of the intensity with no absorber.

(ii) On two occasions overnight runs were made with all conditions normal except that the H.T. voltages on the counters were removed. No counts due to faulty apparatus, electrical pick-up, or other spurious causes, were observed.

(iii) A fast triggered oscilloscope was used to verify that the pulses delivered by the counters, together with the pulses appearing at various points of the circuit, were of the proper shape.

(iv) If the counting rate at the “threshold output” of the threshold amplifier is measured for different bias voltages applied to the discriminating diode, a curve is obtained which consists of a series of downward (with increasing bias) steps (Fig. 6). Along the horizontal portion of the first step all discharges (single or multiple) in the tray of counters are detected; the second step corresponds only to discharges of two or more counters, the third step to three or more, and so on. The lack of complete discontinuity between the steps, and the deterioration in rectangular form as the bias is increased, are due, of course, to imperfect standardization of the pulses. The operating bias is chosen to lie just above the transition between the first step and the second, and it is important that neither the shape of the bias curve in this region, nor the position of the operating point, change appreciably. Such an occurrence would result in not only a change in the effective resolving time for genuine delayed pulses but also the possible registration of spurious delayed pulses due to circuit lags. The dotted curves in Fig. 6 which show the number of spurious delayed counts recorded by the delay mixer (position 1) as a function of bias voltage, indicate the importance of the threshold amplifier stability. Bias curves for both *A* and *B* threshold amplifiers

taken at various times showed that their stability during the experiment was quite adequate.

(v) Two characteristic times are important in determining the sensitivity of the apparatus for the detection of decay particles: the total delay experienced by the triggering pulse (“delay time”), and the resolving time for the delayed coincidence. The former is the time interval between the entrance of a meson and the moment when a decay particle can be first detected; it consists essentially of the sum of two artificially imposed delays, one in the anticoincidence mixer, and one in the triggering channel of the delay mixer. The resolving time is the length of the delayed time interval during which the decay particle can be detected, i.e., the effective gate width of the delay mixer, and is important for the estimation of the casual rate. These times were measured by means of a pulse generator which could supply from separate outputs two pulses whose time separation was adjustable. Thus delayed events could be simulated artificially, and by varying the interval between the pulses the delay time and resolving time were observed. The time separation of a pair of pulses was measured with the fast triggered oscilloscope, whose internal sweep-speed calibrator was checked by independent resolving-time measurements using two random sources with known rates. The delay time is $\sim 1.2 \mu\text{sec.}$; the value of the resolving time, used below for the computation of chance rates, is

$$\tau = 4.7 \pm 0.3 \mu\text{sec.}$$

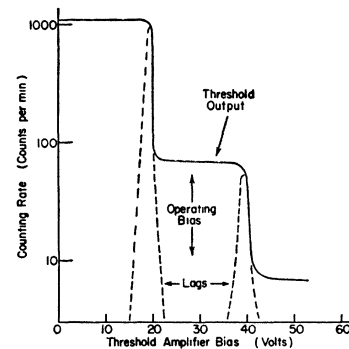


FIG. 6. Bias curve for the threshold amplifier. The dotted curves indicate the number of spurious lags, greater than $\sim 1 \mu\text{sec.}$, which are produced when the bias is varied.

The constancy of these values was confirmed by the appropriate control runs and monitoring rates which have already been described.

(vi) Besides the single rates (*A*), (*B*), (*C*), and the triggering rate $(AB-C)$, to which reference has been made above, knowledge of a number of other (prompt) coincidence and anticoincidence rates is required in order to calculate those rates of chance delayed events which are of significance. Examination of these subsidiary prompt rates also furnished additional evidence that the apparatus was working properly. All rates were measured under circuit conditions approximating

as closely as possible those of the experiment. For example, by means of a three-position switch the anticoincidence mixer could be made to function as a two- or three-channel coincidence mixer, and used to measure either (AB) or (ABC) , without other change. For those coincidence events requiring the discharge of at least two counters of trays A or B (*viz.* (AA) or (BB)), the appropriate "threshold output" was used.

Most of these rates depended somewhat on the thickness of absorber present, and so were measured for various conditions; a typical set of values obtained with the 80 g/cm² lead absorber is given below:^d

$$\begin{aligned}(AB) &= 290 \pm 6/\text{min.} \\ (ABC) &= 249 \pm 6/\text{min.} \\ (AAB-C) &= 2.4 \pm 0.3/\text{min.} \\ (ABB-C) &= 1.6 \pm 0.3/\text{min.} \\ (AABB-C) &= 0.2 \pm 0.1/\text{min.} \\ (AB-C) &= 30.5 \pm 0.3/\text{min.}\end{aligned}$$

The value included for $(AB-C)$ is actually the mean triggering rate for the whole run with the 80 g/cm² lead absorber. These rates will be used in the next section for the computation of the chance rates.

5. Computation of Chance Rates

Because of the importance of a knowledge of the contribution to the $(AB-C)_{\text{del}}$ rate by chance events, and the fact that the estimation of their rate for our arrangement is not as straightforward as usual, we shall discuss the chance rates in some detail.

It should be noted first that the chance delayed single events, which we designate by $(A)_{\text{del}}^{\text{ch}}$, $(B)_{\text{del}}^{\text{ch}}$ and $(C)_{\text{del}}^{\text{ch}}$, are due to *any discharge* in the tray in question that occurs, within the delayed resolving time τ , after a triggering event which does not "kill" the circuit of the associated delay channel. Thus the chance $(A)_{\text{del}}$ rate may be written approximately:

$$(A)_{\text{del}}^{\text{ch}} = [(AB-C) - (AAB-C)] [7/8(A)] \tau.$$

The reduction in the measured triggering rate $(AB-C)$ by subtraction of the term $(AAB-C)$ allows for those triggering events which, since they involve a double discharge in tray A , produce a pulse at the "threshold output" which "kills" the input channel of the delay mixer. They cannot therefore be associated with an $(A)_{\text{del}}$ count. On the other hand not all the events represented by the measured (A) rate can give rise to a chance delay, for a fraction (roughly 1/8), are not detected because of the dead counter.

Similarly, we may write:

$$(B)_{\text{del}}^{\text{ch}} = [(AB-C) - (ABB-C)] [7/8(B)] \tau.$$

On the other hand the chance $(C)_{\text{del}}$ rate is given

^d The meaning of the symbols will be apparent. For example, $(AAB-C)$ refers to those events in which the discharge of at least one counter of tray A is accompanied by the discharge of at least two of tray B , but is unaccompanied by any discharge in tray C .

simply by:

$$(C)_{\text{del}}^{\text{ch}} = (AB-C)(C)\tau.$$

Chance events of the type $(AB)_{\text{del}}$, $(ABC)_{\text{del}}$, or $(AB-C)_{\text{del}}$, are due essentially to mesons traversing the apparatus so as to discharge counters in trays A and B between 1 and 6 $\mu\text{sec.}$ after a triggering event that has "killed" neither A nor B delay channel circuits. Following the reasoning already applied to $(A)_{\text{del}}^{\text{ch}}$ and $(B)_{\text{del}}^{\text{ch}}$, the following expressions may be written:

$$\begin{aligned}(AB)_{\text{del}}^{\text{ch}} &= [(AB-C) - (AAB-C) - (ABB-C) \\ &\quad + (AABB-C)] [(7/8)^2(AB)] \tau, \\ (ABC)_{\text{del}}^{\text{ch}} &= [(AB-C) - (AAB-C) - (ABB-C) \\ &\quad + (AABB-C)] [(7/8)^2(ABC)] \tau, \\ (AB-C)_{\text{del}}^{\text{ch}} &= (AB)_{\text{del}}^{\text{ch}} - (ABC)_{\text{del}}^{\text{ch}} \\ &= [(AB-C) - (AAB-C) - (ABB-C) \\ &\quad + (AABB-C)] [(7/8)^2(AB-C)] \tau.\end{aligned}$$

(The very small term $(AABB-C)$ is properly added in the above expressions because it has otherwise been subtracted twice—as part of $(AAB-C)$ and as part of $(ABB-C)$.)

We give below typical values of the chance rates, calculated for the condition with 80 g/cm² lead absorber.

$$\begin{aligned}(A)_{\text{del}}^{\text{ch}} &= 0.08/\text{hr.} \\ (B)_{\text{del}}^{\text{ch}} &= 0.12/\text{hr.} \\ (C)_{\text{del}}^{\text{ch}} &= 0.39/\text{hr.} \\ (AB)_{\text{del}}^{\text{ch}} &= 0.028/\text{hr.} \\ (ABC)_{\text{del}}^{\text{ch}} &= 0.024/\text{hr.} \\ (AB-C)_{\text{del}}^{\text{ch}} &= 0.0029/\text{hr.}\end{aligned}$$

It is estimated that the error (standard deviation) in the above rates is in each case $\sim \pm 10$ percent.

The occurrence of types of casual delays other than chance events has not been mentioned above, and actually is of little importance in this experiment. Such delays may occur as a result of random time lags in the counter discharges, or because exceptionally slowly-rising pulses from the counters may take an appreciable time to cross the threshold point of the threshold amplifier. Counter lags may contribute slightly to the single delayed rate $(C)_{\text{del}}$, and to a much smaller extent^e to $(A)_{\text{del}}$ and $(B)_{\text{del}}$. On the other hand, a few threshold amplifier lags may be present in the $(A)_{\text{del}}$ and $(B)_{\text{del}}$ rates. However, the chance that two random lags occur simultaneously to produce multiple delayed events ($(AB)_{\text{del}}$, etc.) is quite negligible, and so for these events, which are the significant ones in the experiment, only the chance rates need be considered.

The values of some of the chance rates can be verified experimentally. These checks will be described in the next section.

6. Experimental Results

The measurements made with absorbers of various materials and thicknesses extended over a period of

^e For example, a casual $(A)_{\text{del}}$ event from this cause can only result from a double discharge (AA) , one pulse of which is accidentally lagged.

about 5 months, during which the checks described above in Section 4 were applied to ensure that the apparatus was functioning properly. With a given absorber in position, readings were taken customarily twice a day until a sufficient number of hours of observation had been accumulated.

A list of the absorbers used, together with the measured values of all delayed coincidence rates, is presented in Table II. Here, we have termed "nominal absorber thickness" the thickness of the absorber which is placed between trays *A* and *B*; the "total absorber thickness" is obtained by adding to the "nominal thickness" half the thickness of the carbon source (2.1 g/cm²) plus the thickness of three (two for tray *B*, one for tray *A*) copper counter walls (2.1 g/cm²). Runs with different absorbers were interspersed with short runs with the absorber removed, and all results obtained in these short runs are combined to give the values presented in Table II for the condition "no absorber."

A few points concerning the rates given in Table II are of interest. The rate $(A)_{\text{del}}$ of course changes with absorber. The fact that $(A)_{\text{del}}$ is consistently higher than the rate $(AB)_{\text{del}}$ may be attributed to several causes: (1) decay particles which pass through the dead counter of tray *B* and traverse the absorber to produce a discharge of tray *A*; (2) decay particles from mesons stopped in the counter walls of tray *C* which can "see" tray *A* without intersecting the sensitive area of tray *B*; (3) more chance $(A)_{\text{del}}$ events than chance $(AB)_{\text{del}}$; (4) random lags in *A*. That random lags contribute little may be seen from the fact that the measured

$(A)_{\text{del}}$ rate with the "thick lead" absorber is equal, within the error, to the estimated chance rate.

The constancy of the rates $(B)_{\text{del}}$, $(C)_{\text{del}}$, and thus $(B)_{\text{del}}+(C)_{\text{del}}$, with different absorbers may be observed. The fluctuations in $(B)_{\text{del}}+(C)_{\text{del}}$ are neither large enough, nor systematic enough, to warrant corrections to $(AB-C)_{\text{del}}$. The mean $(B)_{\text{del}}+(C)_{\text{del}}$ rate for the whole experiment is 12.7/hr., of which it is estimated that ~ 9 /hr. are due to decay particles from the graphite source, ~ 1 /hr. are due to decay particles from counter walls, 0.5/hr. are chance events, and the rest are random lags.

The rate $(ABC)_{\text{del}}$ is also constant, at least to within the large statistical uncertainty, throughout the experiment. Since these events should be only of chance origin, their number furnishes a useful check on the correctness of the calculated value $(ABC)_{\text{del}}^{\text{ch}}$. In a total of 2155 hours, 65 $(ABC)_{\text{del}}$ events were counted, or 0.030 ± 0.004 /hr. This rate lies satisfactorily between the estimated extreme values of $(ABC)_{\text{del}}^{\text{ch}} = 0.024$ /hr. with 80 g/cm² lead absorber, and 0.037/hr. with no absorber. Since the ratio $(AB-C)_{\text{del}}^{\text{ch}}/(ABC)_{\text{del}}^{\text{ch}}$ should be equal to the ratio of prompt coincidences $(AB-C)/(ABC)$ (~ 0.12), this experimental check of $(ABC)_{\text{del}}^{\text{ch}}$ also is strong evidence that our value (0.003/hr.) of $(AB-C)_{\text{del}}^{\text{ch}}$ is estimated correctly.^f

Direct evidence that the chance $(AB-C)_{\text{del}}$ rate at least does not greatly exceed our estimate is provided by the results of runs with thick lead absorbers (80 g/cm² and 95 g/cm²). In 369 hours only 2 $(AB-C)_{\text{del}}$ events were registered, while in the same time 9 $(AB)_{\text{del}}$

TABLE II. Delayed coincidence rates measured with various absorbers in arrangement of Fig. 1.

Absorber	Nominal absorber thickness g/cm ²	Total absorber thickness g/cm ²	Hours of observation	$(A)_{\text{del}}$ counts/hr.	$(B)_{\text{del}}$ counts/hr.	$(C)_{\text{del}}$ counts/hr.	$(B)_{\text{del}}+(C)_{\text{del}}$ counts/hr.	$(AB)_{\text{del}}$ counts/hr.	$(ABC)_{\text{del}}$ counts/hr.	$(AB-C)_{\text{del}} = (AB)_{\text{del}} - (ABC)_{\text{del}}$ counts/hr.
No absorber	0	4.2	408	1.56 ± 0.06	4.0	8.5	12.5 ± 0.2	0.82	0.05	0.77 ± 0.05
Carbon	5.1	9.3	67	1.09 ± 0.13	3.7	8.7	12.4 ± 0.4	0.57	0.03	0.54 ± 0.09
Carbon	13.6	17.8	142	0.53 ± 0.06	4.9	9.2	14.1 ± 0.3	0.21	0.04	0.17 ± 0.04
Carbon	16.1	20.3	250	0.34 ± 0.04	4.0	8.3	12.3 ± 0.2	0.12	0.02	0.10 ± 0.02
Carbon (16.1 g/cm ²) + Iron (2.6 g/cm ²)*	18.7	22.9	158	0.21 ± 0.04	4.3	8.7	13.0 ± 0.3	0.08	0.02	0.06 ± 0.02
Carbon (13.6 g/cm ²) + Copper (14.2 g/cm ²)*	27.8	32.0	119	0.18 ± 0.04	4.2	8.3	12.5 ± 0.3	0.08	0.03	0.05 ± 0.02
Aluminum	26.7	30.9	94	0.15 ± 0.04	3.8	7.8	11.6 ± 0.4	0.06	0.02	0.04 ± 0.02
Lead	4.1	8.3	121	0.91 ± 0.09	3.9	7.3	11.2 ± 0.3	0.44	0.02	0.42 ± 0.06
Lead	8.2	12.4	90	0.51 ± 0.08	4.0	10.2	14.2 ± 0.4	0.29	0.01	0.28 ± 0.06
Lead	16.5	20.7	154	0.21 ± 0.04	3.6	10.9	14.5 ± 0.3	0.09	0.04	0.05 ± 0.02
Lead	33.7	37.9	183	0.19 ± 0.03	4.2	8.1	12.3 ± 0.3	0.08	0.04	0.04 ± 0.02
"Thick" lead**		~ 100	369	0.10 ± 0.02	4.1	8.6	12.7 ± 0.2	0.02	0.02	2 in 369 hours

* The maximum thickness of graphite for which there was sufficient space was 16.1 g/cm² (9.5 cm). When it was observed that an appreciable number of $(AB-C)_{\text{del}}$ events were recorded with this thickness, some of the graphite near tray *A* was removed, and replaced by denser material (iron or copper). In this way the total absorber thickness was increased without changing geometry, but at the sacrifice of homogeneity of absorber. However, it is probable that the results obtained in these cases are not very dissimilar to those which would have been obtained had the absorber consisted of the same thickness of pure carbon, for the first part of the decay particle path, where the rate of energy loss is most sensitive to change of *Z*, lies in the carbon as before.

** Combined results from two runs, one of 211 hours with 80 g/cm² lead, and one of 158 hours with 95 g/cm² lead; in both cases the lead was supported by 6 g/cm² steel.

^f Some subsidiary tests, in which the low intensity chance delayed rates were increased by predictable factors to the point where they could be measured without difficulty, also supported the validity of our estimates.

TABLE III. Summary of results obtained with a copper source.

Absorber	Hours of observation	$(AB-C)_{\text{del}}$	
		Total counts	Counts/hr.
No absorber	45	44	1.0
25 g/cm ² lead	197	9	0.05

and 7 $(ABC)_{\text{del}}$ events were registered; all are consistent with the estimated chance rates.

Examination of the last column of Table II shows that the $(AB-C)_{\text{del}}$ rate is of the order of one per day for all absorbers having thicknesses in the range ~ 20 to 40 g/cm². Although these low rates have been measured with very poor accuracy, they are, nevertheless, over ten times the chance rate, and so can only be attributed to a very penetrating radiation associated with the meson decay. The immediate consequences of this result are discussed in the succeeding section, while an investigation of the nature of the penetrating radiation forms the subject of Part II of this paper.

In order to check quickly that the penetrating radiation is not associated *only with the decay of negative mesons*, the carbon source was replaced by a copper one of approximately the same area, and 23 g/cm² thick. Now, since all mesons stopped between trays *B* and *C* are brought to rest in copper (or brass), only radiation from the decay of *positive* mesons⁸ can be responsible for any $(AB-C)_{\text{del}}$ effect observed. The essential results of the measurements with copper source, with and without a 25g/cm² lead absorber, are given in Table III. Since the chance rates are approximately the same as with the carbon source, the observed rate with the lead absorber is evidently a genuine decay effect, and establishes that the penetrating radiation is not exclusively a consequence of negative meson decay.

7. Discussion

The rates $(AB-C)_{\text{del}}$ presented in Table II are plotted against the total absorber thickness in Fig. 7. Here the reality of the existence of the penetrating radiation is apparent, and the distribution of points for all absorbers strongly suggests the division of the decay radiation into two components according to their relative penetration. Thus, for example, the "soft component" is essentially absorbed by about 25 g/cm² carbon; the "hard component," on the other hand, is easily detected after 38 g/cm² lead.

The interpretation of Fig. 7 must be conditioned by the following considerations: (i) The "geometry" of our experimental arrangement is poor—the ratio of thicknesses of absorber presented to decay particles incident normally, and at extreme inclination, is $\sim 1:2.5$; (ii) the statistical accuracy of the points is low because of the low decay particle intensity; (iii) it is inherently difficult to assess the effect of straggling in range of the decay particles due to scattering and to radiative collision (bremsstrahlung) energy losses. While

the possibility of deriving the true energy spectrum of the decay particles is therefore immediately precluded, nevertheless certain observations based chiefly on consideration of maximum ranges can be made.

We shall use for reference the values of rate of energy loss and range for *electrons* of 25 and 50 Mev in different elements which are presented in Table IV. These values are calculated from approximate formulas according to Bloch, and to Bethe and Heitler,²¹ with rough corrections for the Fermi polarization effect.²² The quantities

TABLE IV. Approximate values of energy loss, range, and total energy radiated for electrons of 25 and 50 Mev in various elements. (Calculated with rough formulas of Bloch, Bethe, and Heitler.²¹)

Element Energy E_0 (Mev)	Carbon		Aluminum		Copper		Lead	
	25	50	25	50	25	50	25	50
$-(dE/dx)_{\text{coll}}$ (Mev g ⁻¹ cm ²)	1.8	1.9	1.7	1.9	1.6	1.7	1.3	1.4
$-(dE/dx)_{\text{rad}}$ (Mev g ⁻¹ cm ²)	0.34	0.74	0.70	1.5	1.4	3.0	3.4	7.0
$-(dE/dx)_{\text{tot}}$ (Mev g ⁻¹ cm ²)	2.1	2.6	2.4	3.4	3.0	4.7	4.7	8.4
R_{max} (g cm ⁻²)	14	26	15	27	17	30	19	37
R_{av} (g cm ⁻²)	13	22	12	19	12	18	9.5	13
$(E_0)_{\text{rad}}$ (Mev)	2.1	7.9	4.2	14	7.3	22	13	33

are defined as follows:

$-(dE_0/dx)_{\text{coll}}$ is the average energy loss per unit path length by an electron of energy E_0 due to ionization collisions;

$-(dE_0/dx)_{\text{rad}}$ is the corresponding average energy loss due to radiation;

$-(dE_0/dx)_{\text{tot}} = -(dE_0/dx)_{\text{coll}} - (dE_0/dx)_{\text{rad}}$ is the average total energy loss per unit path length by an electron of energy E_0 ;

$R_{\text{max}} = \int_0^{E_0} \frac{dE}{-(dE/dx)_{\text{coll}}}$ is the maximum range (integrated path length) of an electron of initial energy E_0 (i.e., radiation loss omitted);

$R_{\text{av}} = \int_0^{E_0} \frac{dE}{-(dE/dx)_{\text{tot}}}$ is the average range (integrated path length) of an electron of initial energy E_0 ;

$(E_0)_{\text{rad}}$ is the average total energy lost as radiation by an electron of initial energy E_0 before it comes to rest.

We note first the considerable $(AB-C)_{\text{del}}$ rate observed with a carbon absorber thickness equivalent to

²¹ See H. Bethe and W. Heitler, Proc. Roy. Soc. A **146**, 83 (1934); W. Heitler, *The Quantum Theory of Radiation* (Oxford University Press, London, 1944).

²² E. Fermi, Phys. Rev. **57**, 485 (1940); G. C. Wick, Ricerca Scient. **12**, 858 (1941); O. Halpern and H. Hall, Phys. Rev. **73**, 477 (1948).

the *maximum* range of a 25 Mev electron (14 g/cm²). The two-particle decay hypothesis (Eq. (3)) for which all electrons have a unique energy ~ 25 Mev therefore is untenable. That the observed intensity (~ 0.3 count/hr.) could only be due in small part to bremsstrahlung from 25-Mev electrons may be seen from the following rough argument.^g The total number of decay particles emitted within the solid angle of acceptance of the counters is ~ 0.8 /hr. $((AB-C)_{del}$ rate with no absorber). The average total energy radiated by a 25-Mev electron which starts in the carbon source, traverses the counter walls of tray *B*, and is stopped in the carbon absorber, is estimated to be < 5 Mev. For simplicity, we assume that all photons are emitted in the forward direction, and neglect absorption. The maximum efficiency of a counter for detecting an incident photon is taken to be 1 percent/Mev. (See Part II, Section 7.) The counting rate which can be attributed to bremsstrahlung assuming all decay particles to be electrons of initial energy 25 Mev is therefore

$$< 0.8 \times 5 \times 0.01 = 0.04/\text{hr.}$$

At absorber thicknesses greater than the maximum range of a 50-Mev electron (26 g/cm² carbon), the $(AB-C)_{del}$ rate is ~ 0.04 /hr. This rate we consider to represent the intensity of the "hard component," since it is not reduced very greatly by the introduction of even 38 g/cm² of lead. It might be pointed out here that most of the counting time in the absorption experiments was spent in establishing the reality of the "hard component."

To identify the "hard component" with charged particles is to invoke excessively high energies (e.g., up to 100 Mev or more) which cannot be accounted for by any μ -meson decay process. An alternative explanation is to attribute the effect to a neutral radiation which is associated with the meson decay process or its products, and which can give effects detectable by the counters.

One radiation which does have the required properties to explain qualitatively the "hard component" is the γ -radiation resulting from bremsstrahlung processes suffered by the charged decay particles. It may be noted, in fact, that the points of Fig. 7 suggest a stronger absorption^h of the "soft component" in lead than in graphite; such a phenomenon would indicate a significant radiation loss. It has been shown above that the counting rate to be expected due to bremsstrahlung from 25-Mev electrons is < 0.04 /hr. A similar estimate for electrons of 50 Mev gives an *upper limit* of 0.10 counts/hr. The intensity of the "hard component" is not, therefore, inconsistent with the effect to be expected from bremsstrahlung, assuming that the decay particles are electrons, either negative (carbon source), or positive (carbon and copper sources). Furthermore, it may be noted that the relative intensities measured with

the three thickest lead absorbers, although measured to a very low accuracy, are not in conflict with the expected²¹ absorption coefficient for γ -radiation, which lies in the range 0.45 cm⁻¹–1 cm⁻¹ for all energies between 1 and 50 Mev.

In Part II experiments are described which give strong evidence that the "hard component" is, in fact, bremsstrahlung from the particles constituting the "soft component."

Before passing to the description of these experiments, it may be useful to compare our absorption measurements with those of Steinberger.¹³ As for the "soft component," our results are in agreement with his. Because his intensity was higher than ours (a much larger number of counters was used), Steinberger was able to analyze his absorption curves in more detail than we felt justified in doing. On the other hand, the fact that the casual rate in Steinberger's experiments was much higher than in our experiment made it impossible for him to investigate the "hard component."

PART II. THE BREMSSTRAHLUNG COMPONENT

1. General Considerations

Because of the limitations described in Part I which are attendant on the interpretation of the absorption measurements, and, in particular, of the effect observed with thick absorbers, attention was turned to an investigation of the nature of the "hard component." This work was directed toward determining two points: (1) whether or not a neutral radiation is responsible for the great penetrating power of the "hard component," and (2) the dependence of the observed intensity of the "hard component" on the atomic number of the absorber. Furthermore it evolved, from the results of these investigations, that it was possible to derive information on the mass of the charged decay particles from considerations of their radiative power.

The method used to investigate question (1) was

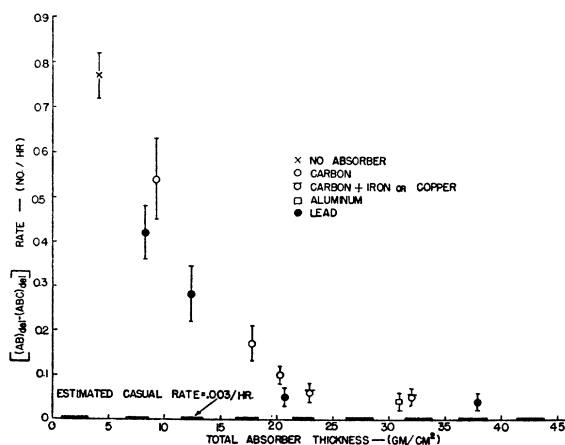


Fig. 7. Results of the absorption measurements. The $(AB-C)_{del}$ rates are plotted against the total absorber thickness for each element used.

^g A more detailed consideration of this problem is given in Part II.

^h For more conclusive evidence see Part II.

essentially to divide the (thick) decay particle absorber by an intermediate tray of counters. It is then possible to see whether or not a delayed coincidence due to the hard component (i.e., detected entering and leaving the total thick absorber) is accompanied by a discharge of the intermediate tray. Now, since the efficiency of the intermediate tray for detecting a charged decay particle must be high, the type of geometry (Fig. 1) used for the absorption measurements is unsuitable. Thus the possibility that the decay particle passes through a counter which has been rendered insensitive by the

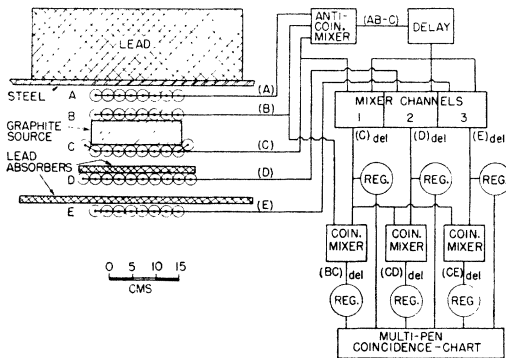


FIG. 8. Experimental arrangement for the detection of bremsstrahlung, with simplified block diagram of the circuits. The lengths of the counters and source are ~ 40 cm.

incoming meson itself, giving by the absence of a pulse from the intermediate tray an apparent but false anti-coincidence, must be avoided. To do this the counters used to detect decay particles must be distinct from those used to detect the stopped mesons; the former have therefore been placed below the source for this experiment, and they detect decay particles travelling in a downward direction.

To observe the Z dependency of the "hard component," a similar arrangement of counters was used in which absorbers of carbon and lead could be interchanged with a minimum disturbance of the apparatus in every other respect.

A description of the counter arrangement, decay particle source, and counting apparatus, which is applicable to both experiments reported in Part II, is given in the next section.

2. Apparatus

The disposition, and function of the apparatus used in these experiments may be understood by referring to Fig. 8, in which the left-hand side shows the arrangement of counters and source (variations in the distances between counter trays C , D , and E , and in the absorbers occupying these spaces will be described later), and the right-hand side is a simplified block diagram of the counting circuits. Cathode-followers, wave-front amplifiers, and a threshold amplifier for tray B , have been omitted for simplicity (compare Figs. 1 and 3).

The counters used—15-inch copper counters in trays A and B , 16-inch brass counters in trays C , D , and E —are described in Part I, Section 2. In trays C and D the aluminum shelves that support the counters have been cut away opposite the sensitive areas of the latter, so that there is no solid material between the source and tray E other than the counter walls and the absorbers which may be inserted. The individual electronic circuits are described in Part I, Section 3.

Mesons stopped in the graphite source ($20 \text{ cm} \times 40 \text{ cm} \times 8.5 \text{ g/cm}^2$ thick) are detected by the anticoincidence ($AB-C$) as before. The delayed coincidence events (C)_{del}, (D)_{del}, or (E)_{del}, which may be due to a decay particle traversing trays C , D , or E between 1 and 6 microseconds after a meson stops, are selected by the three channels of the delay mixer. The outputs of these channels are mixed in pairs in two-channel coincidence mixers in order to observe events of the type (CD)_{del} and (CE)_{del}. A third two-channel mixer accepts pulses from the first channel of the delay mixer ((C)_{del} pulses) and from the "threshold output" from B , and therefore effectively detects events of the type (BC)_{del}. The (BC)_{del}, (CD)_{del} and (CE)_{del} pulses are recorded by different pens of an Esterline-Angus ten-pen "Operation Recorder" with a chart speed of 4 inches/hr. Since the rates of these pulses are always small (a few per hour, or less), it is convenient to detect coincidences or anticoincidences between these events by observing their correlation in time on the chart. We shall therefore refer to the ten-pen recorder as the "coincidence chart."

The events (BC)_{del} are recorded in order to reduce the chance rate of delayed coincidences for the three lower trays; thus if an event (C)_{del}, (D)_{del} or (E)_{del} is accompanied by a discharge of tray B , we attribute it to the chance passage of a second meson, and disregard it. The significant delayed events defined with reference to the records on the coincidence chart are listed below: ($CD-B$)_{del} refers to all (CD)_{del} pulses non-coincident with a (BC)_{del} pulse; ($CE-B$)_{del} refers to all (CE)_{del} pulses non-coincident with a (BC)_{del} pulse; ($CDE-B$)_{del} refers to those (CE)_{del} pulses which are coincident with a (CD)_{del} pulse, but non-coincident with a (BC)_{del} pulse; ($CE-D-B$)_{del} refers to those (CE)_{del} pulses which are non-coincident with either a (CD)_{del} pulse or with a (BC)_{del} pulse. The more frequent delayed events (C)_{del}, (D)_{del}, and (E)_{del} are also recorded separately on the chart, so that their time-distribution can be observed. Finally, another pen is used to indicate mains power failure.

3. Control Measurements

The various control measurements, and checks of the proper functioning of the apparatus, were essentially similar to those described in Part I, Section 4. They are listed briefly below, with comments only in those cases where there are significant differences from the procedures or data of Part I.

(a) *Continuous Checks.* (i) The triggering events ($AB-C$) were counted continuously. The rate was between 75/min. and 80/min. for all runs, and, as expected, was not influenced by the absorbers. That the triggering rate is much higher than in Part I is due mainly to the smaller separation of trays A and B .

(ii) The rate $(C)_{\text{del}}$ was used as an over-all check of the "source strength," and sensitivity of the apparatus. No significant variations in this rate (18/hr.) were observed for all runs in which absorbers were present between trays C and D , and D and E ; with these absorbers removed there were indications of a slight decrease (~ 1 /hr. or less). This difference might be explained as being the contribution to $(C)_{\text{del}}$ from mesons which "leak" past tray C and decay in the absorber. In the absence of the source (and absorbers) the $(C)_{\text{del}}$ rate was ~ 3 /hr. of which we estimate that 0.5/hr. are chance, 0.5-1/hr. are due to decay particles from mesons stopped in counter walls, and the balance may be attributed to random counter lags.

(iii) All coincidence chart records were examined for evidence of spurious events or improper mixing.

(b) *Periodic Checks.* (i) The single counting rates for the separate trays were checked daily. Their magnitudes are illustrated by the following mean values obtained during the experiment described in Section 6 below (see Fig. 9, I or II); they are somewhat different for other variations of this geometry, or if the absorbers are removed.

$$\begin{aligned}(A) &= 1015/\text{min.} \\ (B) &= 1060/\text{min.} \\ (C) &= 1585/\text{min.} \\ (D) &= 1560/\text{min.} \\ (E) &= 1285/\text{min.}\end{aligned}$$

(ii) Checks of voltages and pulse shapes were made as described in Part I.

(c) *Occasional Checks.*—(i) Check runs made with no decay particle absorbers will be referred to later. In each arrangement (Section 5, Section 6, below) a short run was made with the source removed as well, to verify that most of the counts which are attributed to decay particles disappeared.

(ii) Several of the occasional check measurements described in Part I were not made during this part of the work. They were felt to be unnecessary since (a) the apparatus was checked carefully at the beginning,

TABLE V. Chance rates computed for the experimental arrangements of Part II.

Type of event	Arrangements for the detection of neutral radiation (Section 5)		Arrangements I and II for testing the Z dependence (Section 6) counts/hr.
	Lead below C counts/hr.	Carbon below C counts/hr.	
$(C-B)_{\text{del}}^{\text{ch}}$	0.4 \pm 0.1	0.5 \pm 0.1	0.5 \pm 0.1
$(CD-B)_{\text{del}}^{\text{ch}}$	0.11 \pm 0.01	0.09 \pm 0.01	0.10 \pm 0.01
$(CE-B)_{\text{del}}^{\text{ch}}$	0.08 \pm 0.01	0.05 \pm 0.01	0.06 \pm 0.01
$(CDE-B)_{\text{del}}^{\text{ch}}$	0.07 \pm 0.01	0.05 \pm 0.01	0.06 \pm 0.01
$(CE-D-B)_{\text{del}}^{\text{ch}}$	0.006 \pm 0.001	0.004 \pm 0.001	0.004 \pm 0.001

(b) the runs described in Section 5 took a relatively short time, and (c) the measurements in Section 6 consisted of the periodic alternation of two conditions which were to be compared.

(iii) The various prompt coincidence rates required for computation of the chance delayed rates were measured for each variation of counter-absorber geometry. The typical set of rates given below applies to Section 6 (I and II); they would be somewhat different for the counter tray separations used in Section 5.

$$\begin{aligned}(ABB-C) &= 11 \pm 1/\text{min.} \\ (BC) &= 445 \pm 11/\text{min.} \\ (CD) &= 487 \pm 10/\text{min.} \\ (CD-B) &= 202 \pm 7/\text{min.} \\ (CE) &= 267 \pm 7/\text{min.} \\ (CE-B) &= 117 \pm 5/\text{min.} \\ (CE-D) &= 10.4 \pm 1.0/\text{min.} \\ (CE-D-B) &= 3.6 \pm 0.5/\text{min.}\end{aligned}$$

$$(AB-C) = 78 \pm 1/\text{min. (mean triggering rate).}$$

Other rates required may be derived from the above; for example,

$$\begin{aligned}(BCDE) &= (CE) - (CE-B) \\ &\quad - (CE-D) + (CE-D-B), \text{ etc.}\end{aligned}$$

4. Computation of Chance Rates

As in Part I, a knowledge of the chance rates of delayed coincidences of different types is essential in order to interpret the results correctly. Moreover, since in the most significant cases they are too low to measure easily, calculated values must be used. A discussion of the formulas which were used follows.

It should be noted that, for the arrangement shown in Fig. 8, corrections for dead counters and for instrumental dead-times are introduced only when trays B or D cancel chance delayed events. Thus chance rates as $(C)_{\text{del}}^{\text{ch}}$, $(D)_{\text{del}}^{\text{ch}}$, $(E)_{\text{del}}^{\text{ch}}$, $(CD)_{\text{del}}^{\text{ch}}$, $(CE)_{\text{del}}^{\text{ch}}$, etc., are given accurately by such expressions as

$$\begin{aligned}(C)_{\text{del}}^{\text{ch}} &= (AB-C)(C)\tau, \\ (CD)_{\text{del}}^{\text{ch}} &= (AB-C)(CD)\tau,\end{aligned}$$

etc. On the other hand $(C-B)_{\text{del}}^{\text{ch}}$, $(CD-B)_{\text{del}}^{\text{ch}}$, $(CDE-B)_{\text{del}}^{\text{ch}}$ are given only *very approximately* by the simple relations:

$$\begin{aligned}(C-B)_{\text{del}}^{\text{ch}} &\sim (AB-C)(C-B)\tau, \\ (CD-B)_{\text{del}}^{\text{ch}} &\sim (AB-C)(CD-B)\tau, \\ (CDE-B)_{\text{del}}^{\text{ch}} &\sim (AB-C)(CDE-B)\tau,\end{aligned}$$

TABLE VI. Delayed coincidence rates with arrangement of Fig. 8—lead below C.

Condition	Hours of observation	$(CD-B)_{\text{del}}$ counts/hr.	$(CE-B)_{\text{del}}$ counts/hr.	$(CDE-B)_{\text{del}}$ counts/hr.	$(CE-D-B)_{\text{del}}$ counts/hr.
Without absorbers measured	21	9.0 \pm 0.7	4.8 \pm 0.5	4.6 \pm 0.5	~ 0.2 (3 counts)
With absorbers measured	103	0.56 \pm 0.08	0.19 \pm 0.05	0.09 \pm 0.03	0.10 \pm 0.03
Estimated chance	—	0.11 \pm 0.01	0.08 \pm 0.01	0.07 \pm 0.01	0.006 \pm 0.001

TABLE VII. Delayed coincidence rates with arrangement similar to Fig. 8—carbon below C.

Condition	Hours of observation	$(CD-B)_{del}$ counts/hr.	$(CE-B)_{del}$ counts/hr.	$(CDE-B)_{del}$ counts/hr.	$(CE-D-B)_{del}$ counts/hr.
Without absorbers measured	67	5.0 ± 0.3	2.6 ± 0.2	2.4 ± 0.2	0.15 ± 0.05
With absorbers measured	90	0.96 ± 0.10	0.19 ± 0.05	0.06 ± 0.03	0.13 ± 0.04
Estimated chance	—	0.09 ± 0.01	0.05 ± 0.01	0.05 ± 0.01	0.004 ± 0.001

for after a triggering event ($AB-C$) we find *either* one dead counter in tray B which is impotent to cancel a delayed event, *or* a dead circuit in the $(BC)_{del}$ mixer (if two or more B counters fired) so that the whole B tray is ineffective for subsequent canceling. It follows then that, for example, $(CDE-B)_{del}^{ch}$ is given very closely by

$$(CDE-B)_{del}^{ch} = \langle [(AB-C) - (ABB-C)] \times [(CDE) - 7/8(BCDE)] + (ABB-C)(CDE) \rangle \tau,$$

and similarly for other expressions containing $-B$.

The evaluation of the important rate $(CE-D-B)_{del}^{ch}$ is even more elaborate, and a detailed formulation will not be given here. We shall, however, describe the two chance sequences of events which contribute chiefly to the effect. First, a triggering event ($AB-C$) may be followed by a chance ($CE-D-B$) (e.g., by a meson which misses tray B , discharges C , "leaks" through D , and discharges E). Alternatively, a triggering event of the type ($ABD-C-E$) (e.g., a meson discharges trays A and B , "leaks" through C , discharges D (whose circuit has a long dead-time), and misses E), is followed by a chance ($CE-B$). The contributions to $(CE-D-B)_{del}^{ch}$ from both of these effects have been estimated, taking into account the corrections for dead counters and dead circuits, and turn out to be of comparable magnitude. Effects due to other combinations of events, in particular those due to the chance

TABLE VIII. Delayed coincidence rates for the two arrangements of Fig. 9 (corrected for chance events).

Arrangement	Hours of observation	$(CD-B)_{del}^{net}$ counts/hr.	$(CE-B)_{del}^{net}$ counts/hr.	$(CE-D-B)_{del}^{net}$ counts/hr.
No absorbers	47	5.7 ± 0.4	1.8 ± 0.2	0.11 ± 0.05
I. Carbon below C	392	1.50 ± 0.07	0.02 ± 0.02	0.046 ± 0.013
II. Lead below C	392	1.02 ± 0.06	0.01 ± 0.02	0.13 ± 0.02

coincidence of *three* independent events within the resolving time, are much smaller, and are neglected.

The computed values of chance rates for the more important delayed events are listed in Table V; the three columns of values are applicable to the two variations in geometry described in Section 5, and to the variation used in Section 6 (with either absorber arrangement I or II). The resolving time has been taken as $4.7 \pm 0.3 \mu\text{sec.}$ —the value used in Part I.

5. Detection of Neutral Radiation

In the first experiment designed to test whether a neutral radiation is responsible for the "hard component," the particular arrangement of absorbers shown in Fig. 8 was used. The separation between trays C and D (center to center) is 5.4 cm; that between trays D and E is 6.8 cm. The absorbers between trays C and D , and D and E , each consist of 16.5 g/cm² lead. These absorber thicknesses were chosen in order to prevent most of the "soft component" from reaching tray D , and at the same time to allow an appreciable intensity of "hard component" to be detected by tray E (see Fig. 7). Runs were made both with and without these two absorbers, and the measured rates of importance, together with the estimated chance rates for the condition "with absorbers," are given in Table VI.

It will be readily seen that the relative contributions of $(CDE-B)_{del}$ counts and $(CE-D-B)_{del}$ counts to the total $(CE-B)_{del}$ rate are quite different for the two conditions. Without absorbers, nearly all $(CE-B)_{del}$ events are accompanied by a discharge of D : the three $(CE-D-B)_{del}$ events represent about the fraction to be expected as a result of the geometrical transparency of the D tray. On the other hand, taking into account the expected chance rates calculated in Section 4 (Table V), and shown again in Table VI for comparison, it is apparent that with absorbers present few, if any, of the $(CE-B)_{del}$ decay events are accompanied by discharges of tray D . This demonstrates the production in the first part of the absorber (between C and D) of a neutral radiation which can traverse tray D without discharging it, but which may subsequently give rise to an ionizing radiation detected by tray E .

In order to establish the same character of the "hard component" in the case of low Z absorbers, a variation of the above experiment was carried out with the lead between C and D replaced by 13.6 g/cm² carbon. To accommodate the greater absorber thickness, the distance between trays C and D was increased to 13.0 cm.

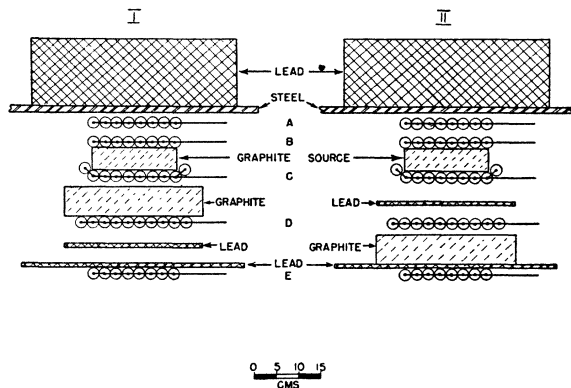


FIG. 9. Two arrangements which were alternated to compare the production of bremsstrahlung in carbon (I) and in lead (II). The circuits are identical to those indicated in Fig. 8.

The absorber between D and E was 16.5 g/cm² lead as before, with a D - E tray separation of 7.1 cm. The results of runs with and without the carbon and lead absorbers, and the estimated chance rate with absorbers, are presented in Table VII.

The data for carbon again demonstrate the presence of a neutral radiation in the "hard component." In view of both these results, the attribution of the "hard component" to bremsstrahlung from the particles of the "soft component" becomes very plausible.

6. Z Dependency of the "Hard Component"

The strong dependency on the atomic number of the stopping material which is characteristic of the bremsstrahlung process should provide a good test of the nature of the "hard component." Thus we see from Table IV that electrons of 25-50 Mev stopped in lead lose on the average more than half their energy by radiation; in carbon, on the other hand, most of their energy loss is by ionization. By comparing the intensities of the "hard component" with lead and carbon absorbers, under conditions in which changes in such factors as the geometry, the absorption of the "hard component," the sensitivity of the counters, etc., are reasonably constant, we can therefore determine whether they are consistent with those to be expected from bremsstrahlung. It should be noted that no attempt was made to keep these factors constant for the two arrangements already used which were described in the preceding section.

The two alternate arrangements of counters and absorbers chosen for comparison are shown in Fig. 9. Here the location of the counter trays is kept fixed, and lead and graphite absorbers are interchanged in position to give alternately the two sequences of counters and absorbers:

- I. Tray C —11.0 g/cm² carbon—Tray D —8.2+8.2 g/cm² lead—Tray E ;
- II. Tray C —8.2 g/cm² lead—Tray D —11.0 g/cm² carbon+8.2 g/cm² lead—Tray E .

The circuits are those already shown in Fig. 8, and the operation of the apparatus has been described in Section 2 (Part II). A few points of particular significance for this experiment will be discussed.

It is convenient to use now the $(CE-D-B)_{del}$ rate as a measure of the "hard component" intensity. We conclude from the results of Section 5 that little or no intensity is sacrificed by doing this; on the other hand the fact that the chance rate for this type of event is so low is an indispensable advantage.

The selection and location of the absorbers is based on the following considerations. An 8.2 g/cm² thickness of lead is kept immediately above tray E for both arrangements I and II. The combination of lead and counters may then be considered together as a photon detector whose sensitivity is fairly independent of the other absorbers immediately above it. The result of the

TABLE IX. Estimated $(CE-D)_{del}^{rad}$ rates due to bremsstrahlung for the two arrangements of Fig. 9.

Particles	$(CE-D)_{del}^{rad}$, counts/hr.		Ratio: II/I
	Arrangement I	Arrangement II	
Electrons { 25 Mev	0.015	0.037	2.5
{ 50 Mev	0.043	0.12	2.8
"Heavy electrons," { 25 Mev	0.004	0.015	4
mass = $2m_e$ { 50 Mev	0.012	0.06	5

alternation in positions above and below D of the graphite absorber (11.0 g/cm²) and the other lead absorber (8.2 g/cm²) means that the events $(CE-D-B)_{del}$ are due in the one case (I) to neutral radiation produced in carbon, and in the other (II) to neutral radiation produced in lead. At the same time, the total absorbing material between C and E is kept constant. While neither carbon nor lead absorber between C and D is of sufficient thickness to completely remove the "soft component," the fraction left should be sufficiently degraded in energy that it cannot contribute much to the average total radiation (bremsstrahlung), and moreover, because of its penetration, it cannot have suffered appreciable radiation loss in the absorber above D . The significance of this will be seen below. The lead and carbon thicknesses were chosen (see Fig. 7) to stop roughly the same fraction of the "soft component" between C and D in the two arrangements. The lead is placed either above or below tray D at positions which correspond roughly to the center of the graphite in the alternative arrangement.

The positions of the graphite and lead absorbers were reversed about every three days, for a period of about one month. All check readings indicated that the apparatus behaved consistently throughout. A single run was made with all absorbers between C and E (including the lead immediately above E), removed. A summary of the important rates, from which the appropriate chance rates derived in Section 4 (Table V) have already been subtracted, is given in Table VIII.

The ratio of the $(CE-D-B)_{del}^{net}$ rate for arrangement II to that for arrangement I is 2.8 ± 0.9 . It will be shown in Section 7 that the $(CE-D-B)_{del}^{net}$ rates, and in particular their ratio, are consistent with the values to be expected if the neutral radiation is bremsstrahlung from electrons.

The $(CD-B)_{del}^{net}$ rates for arrangements I and II (Table VIII) are due essentially to the "soft component." We observe that the latter is, in fact, more strongly absorbed by 8.2 g/cm² lead than by 11.0 g/cm² carbon, as would be expected if the particles suffer appreciable radiation loss.

7. Discussion

We have estimated the $(CE-D-B)_{del}^{net}$ counting rates to be expected for the two arrangements described in Section 6 as a result of bremsstrahlung assuming that the radiating particles are electrons, responsible for

the observed "soft component" of the absorption curve. Estimates are made for initial electron energies of both 25 Mev and 50 Mev.

A fairly straightforward evaluation of the effect may be based on the fact that the efficiency of a counter for detection of a photon of energy E is approximately proportional to E .²³ This is true except for energies well below 1 Mev, and provided that the thickness of the counter wall is not less than the maximum range of the secondary Compton or pair electrons. In our case the fraction of the energy radiated which is accounted for by photons of <1 Mev is very small because of the form²¹ of the radiation spectrum. It should also be noted that in each arrangement there is 8.2 g/cm² lead immediately above tray E . If ϵ (Mev⁻¹) is the efficiency of tray E (with the lead above) for detecting an incident photon per Mev of photon energy, N the number of electrons per hour of initial energy E_0 whose radiation may be assumed to travel in the direction of tray E , and $(E_0)_{\text{rad}}$ the average total energy (Mev) radiated per electron in the material above tray D , then the $(CE-D)_{\text{del}}$ rateⁱ due to bremsstrahlung may be written approximately

$$(CE-D)_{\text{del}}^{\text{rad}} = \alpha \epsilon N (E_0)_{\text{rad}} \text{ counts/hr.}$$

The factor $\alpha (<1)$ accounts for the effective reduction in intensity due to absorption of the photons by the material between their point of origin and tray E . It may be approximated by the quantity $e^{-\tau_1 x_1 - \tau_2 x_2}$, where τ_1 is a suitable average value of absorption coefficient in carbon over the energy range of the photons, x_1 is a suitable average value of the thickness of the carbon effective for absorption, and τ_2 , x_2 are similar quantities for the lead. We have taken²¹ for τ_1 , 0.03 g⁻¹ cm², and for τ_2 , 0.06 g⁻¹ cm². Since most of the radiative energy loss takes place in the uppermost part of the absorber between C and D , we cannot be greatly in error by taking for x_1 and x_2 the total thicknesses of carbon and lead respectively between C and E . It follows that α is approximately 0.3 for both arrangement I and arrangement II.

For ϵ we assume the value 0.01 Mev⁻¹ to be appropriate for a counter with lead wall.²³

If the angular spreading of the radiation is neglected, then N will be just the rate $(CDE)_{\text{del}}$ measured with no absorber, i.e., the rate of emission of decay electrons from the source, with appropriate delay, which travel in the direction of tray E . We consider this value to be reasonable since the angular divergence of bremsstrahlung at high energies is small,²¹ and the loss in intensity due to the deviation of emitted photons from the paths of electrons directed towards tray E is partially compensated by the detection of photons produced by electrons traversing C but not directed

towards E . It should be noted that if an electron penetrates the absorber between C and D , and discharges tray D , then any radiation which it may have emitted cannot contribute to the $(CE-D)_{\text{del}}^{\text{rad}}$ effect. The number of such electrons can be estimated and a small correction made for this loss.

Values of $(E_0)_{\text{rad}}$ are estimated in the following manner. Each electron is assumed to start with initial energy E_0 at the center of the source, and to travel always in a direction normal to the counter trays and absorbers. The average energy lost by both radiation and ionization in half the source thickness is computed, giving the average reduced energy E_1 with which the electron enters the C counter walls. Further estimates of radiation and ionization loss in the average thickness of brass in tray C give the average energy E_2 after traversing C . The total energy radiated by an electron of energy E_2 when stopped in carbon (arrangement I) or lead (arrangement II) is finally estimated. The various radiation energy losses are totalled to give $(E_0)_{\text{rad}}$. The values used for rate of energy loss by ionization and by radiation, and of total energy radiated, are derived from the formulas of Bloch, and Bethe-Heitler;²¹ some of these values are given in Table IV.

The expected values $(CE-D)_{\text{del}}^{\text{rad}}$ for electrons with $E_0 = 25$ Mev and $E_0 = 50$ Mev, and for the two arrangements of Section 6 (Fig. 9), are given in Table IX.

It is difficult to evaluate the accuracy to be attached to these estimated rates; we believe they are at least correct to within a factor 2. However the ratio of the two rates for arrangements I and II is known to much better accuracy, for in this case the quantities α , ϵ , and N are not involved, and, because of the similarity in geometry between arrangements I and II, the ratio of counting rates becomes essentially equal to the ratio of the total energies radiated. Moreover this ratio is fairly insensitive to the initial electron energy in the range 25-50 Mev.

A comparison of the experimental values $((CE-D-B)_{\text{del}}^{\text{net}})$, Table VIII) with the values in Table IX shows that both the counting rates observed in arrangements I and II, and their ratio, are consistent with the rates to be expected due to bremsstrahlung from electrons of 25-50 Mev.^j The agreement in the values of the ratio is the stronger since, as indicated above, fewer assumptions are involved in deriving the estimated figure. It may be significant that the rates themselves are closer to those computed for 50-Mev electrons than for 25 Mev. This would indicate that the average energy is in fact greater than 25 Mev, but more quantitative estimates would not be justified.

The total energy lost by radiation by fast particles with a given charge and energy (or momentum) depends

²³ See, for example, Fowler, Lauritsen, and Lauritsen, Rev. Mod. Phys. 20, 236 (1948); Bradt, Gugelot, Huber, Medicus, Preiswerk, and Scherrer, Helv. Phys. Acta 19, 77 (1946).

ⁱ It is superfluous here to indicate that tray B is not discharged.

^j A similar calculation for the absorption experiment (Part I) shows that bremsstrahlung should give a "background" effect of about the magnitude of the "hard component."

very sensitively on their mass. It is possible to conclude from this consideration that the decay particles that radiate in our apparatus are indeed electrons, or, more precisely, that they cannot have a mass much greater than one electron mass. In Table IX we have included values which were calculated for the hypothetical case of particles similar to electrons but with twice the mass ($M=2m_e$). Such "heavy electrons" could hardly produce the amount of bremsstrahlung observed, and of course hypothetical particles with $M>2m_e$ are discriminated against even more strongly. It is reasonable, therefore, to conclude that the charged decay particles are truly electrons, as is generally postulated. The evidence presented here based on their radiative property, is more decisive than evidence from their ionization in a cloud chamber or photographic plate. For example, Leighton, Anderson, and Seriff¹⁸ recently obtained from cloud-chamber evidence a value of $10m_e$ for the upper limit of the mass of the charged decay particles. A similar case analyzed by Fletcher and Forster²⁴ gave a high probability (0.95) that the mass is less than $7m_e$.

Finally it may be pointed out why bremsstrahlung was not observed in some other experiments¹⁰ designed to detect photons associated with the meson decay. The present authors, for example, looked without success for photons in coincidence with decay electrons in order to test a hypothetical electron-photon decay process (Eq. (2)). The counter arrangement for this experiment could only detect a photon travelling in approximately the opposite direction to the electron; it would thus not detect photons from the bremsstrahlung process, which are strongly concurrent in direction with the electrons. The same directional property would also make the bremsstrahlung difficult to observe in the arrangements of Sard and Althaus, and of Piccioni. In these experiments a photon from the "source" is first required to traverse an anticoincidence row of counters, and the probability that these would be discharged by the accompanying electron would be high for a "radiation" photon. In the present experiment this concurrence in direction of electron and photon is allowed, and in fact constitutes one of the arguments for the interpretation we have placed on our results.

CONCLUSIONS

Our study of the absorption of the charged particles emitted in the meson decay process, and the identification of a very penetrating "background" component with the photons resulting from the bremsstrahlung process, have lead to the following conclusions:

(1) The charged particles themselves are electrons, for if they were heavier (mass $2m_e$ or more) it would be difficult to account quantitatively for the observed

intensity of the bremsstrahlung, and for the ratio of the intensities of such radiation produced in lead and carbon;

(2) The absorption curve obtained with carbon absorbers shows conclusively that at least a considerable number of electrons are emitted with energies greater than 25 Mev;

(3) A comparison of measured with calculated intensities of bremsstrahlung indicates that the *average* electron energy is greater than 25 Mev;

(4) The presence of bremsstrahlung obscures the observation of the *maximum* electron energy by absorption measurements. However, it is clear that to interpret our absorption curves, as well as those of Steinberger,¹³ there is no need to invoke the presence of electrons of energy greater than ~ 50 Mev.

The above conclusions referring to the energy of the charged particles are consistent with the extensive data recently obtained by Steinberger¹³ (absorption technique), by Thompson⁴ (cloud chamber), and by Leighton, Anderson and Seriff¹⁸ (cloud chamber).

Our main conclusion referring to the mass of the charged decay particles excludes the possibility that a new type of meson (charged light meson or λ -meson) is emitted in the 2.2- μ sec. decay, and adds to the body of evidence in support of the "electron+2 neutrinos" process (Eq. (5)), requiring a spin $\frac{1}{2}\hbar$ for the μ -meson. This evidence is summarized below with selected references:

(a) There is only one charged particle emitted in the 2.2- μ sec. decay (Thompson, reference 4).

(b) The charged particle is an electron (present work).

(c) There are no high energy photons emitted in the 2.2- μ sec. decay (reference 10).

(d) The charged particles are emitted with an apparently continuous distribution of energies extending up to about 55 Mev (reference 13 and especially 18).

(e) Assuming an "electron+2 neutrinos" process, the mass of the decaying meson can be calculated from the maximum energy of the decay electrons; the value obtained appears to be in very good agreement with the mass of the μ -meson measured²⁵ by other methods (reference 18).

(f) The average energy and the form of the energy spectrum of the decay electrons are, within the accuracy of theory and experiments, in agreement with theoretical expectations²⁶ for the "electron+2 neutrinos" process (reference 18).

(g) The discussions²⁷ of the experiments²⁸ on the production and on the nuclear capture of negative μ -mesons strongly suggest that their spin is $\frac{1}{2}\hbar$.

²⁵ A. S. Bishop, Phys. Rev. **75**, 1468 (1949); R. B. Brode, Rev. Mod. Phys. **21**, 37 (1949).

²⁶ J. Tiomno and J. A. Wheeler, Rev. Mod. Phys. **21**, 144 (1949).

²⁷ B. Pontecorvo, Phys. Rev. **72**, 246 (1947); R. Serber, Phys. Rev. **75**, 1459 (1949); J. Tiomno and J. A. Wheeler, Rev. Mod. Phys. **21**, 153 (1949); R. E. Marshak, Phys. Rev. **75**, 700 (1949).

²⁸ Lattes, Occhialini, and Powell, Nature **160**, 453 and 486 (1947), and see also reference 17; E. Gardner and C. M. G. Lattes, Science **107**, 270 (1948); E. Gardner, Phys. Rev. **75**, 1468 (1949); A. S. Bishop, Phys. Rev. **75**, 1468 (1949); C. M. G. Lattes, Phys. Rev. **75**, 1468 (1949); O. Piccioni, reference 10; Sard, Ittner, Conforto, and Crouch, Phys. Rev. **74**, 97 (1948); W. Y. Chang, Rev. Mod. Phys. **21**, 166 (1949).

²⁴ J. C. Fletcher and H. K. Forster, Phys. Rev. **75**, 204 (1949).

ACKNOWLEDGMENTS

We are deeply indebted to Mr. G. B. Parkinson for designing and supervising the construction of the delay mixer. Mr. F. MacDonald assisted us greatly in constructing the delay mixer, as well as other electronic

apparatus. We wish to thank Miss E. Mooney and Miss C. Walker for their help in taking readings and checking the apparatus during the experiment. Finally, we acknowledge gratefully the interest and encouragement given by Dr. B. W. Sargent and Dr. W. B. Lewis.

A Study of the Spectra of Columbium and Molybdenum in the Extreme Ultraviolet

GEORGE W. CHARLES*

Mendenhall Laboratory of Physics, Ohio State University, Columbus, Ohio

(Received August 31, 1949)

The spectra of columbium and molybdenum in the range 100–1000Å have been investigated. Spectrograms were obtained with a three-meter grazing incidence vacuum spectrograph having a dispersion of 1.0Å/mm at 500Å. The lines of Cb V and Mo VI previously reported have been remeasured. Attempts to find higher members of the series $4d-np$ and $4d-nf$ have proved fruitless except for the transition $4d-6p$ in Mo VI, for which tentative identification is given. Six low levels of Cb VI and Mo VII have been identified by extrapolation of frequencies in the Kr sequence. Some of the classifications are supported by considerations from theory. By applying a Rydberg formula to the transitions $4p^6-4p^5s$ and $4p^6-4p^5d$, the absolute value of the ground level of Cb VI is estimated to be 829,750 cm^{-1} and that of Mo VII is estimated to be 1,020,460 cm^{-1} .

The Br sequence has been extended to Cb VII and Mo VIII. The separations of the ground doublets were predicted by use of

the regular doublet law. Forty-one lines of Cb VII and forty-two lines of Mo VIII have been identified by extrapolation of frequencies and application of the regular doublet law. These lines arise from transitions between the ground doublet arising from $4s^24p^6$ and the configurations $4s^24p^44d$, and $4s^24p^45s$. The absolute values of the $^2P^{\circ}_{3/2}$ ground levels of Cb VII and Mo VIII are estimated to be 1,005,000 cm^{-1} and 1,235,000 cm^{-1} , respectively.

Results of an approximate calculation of the energy levels of the configuration p^4s in intermediate coupling are given and are compared with the observed levels in Cb VII and Mo VIII. The order of J -values is, with one exception, the same for the calculated levels as for the observed levels. The two sets of levels agree roughly, although the observed levels are more intimately mixed than the calculated levels.

INTRODUCTION

THE spectra of columbium have previously been investigated through Cb V and those of molybdenum through Mo VI (with the exception of Mo III).¹ In the present study, some of the low lying levels of higher stages of ionization of these metals are identified on the basis of extrapolations along isoelectronic sequences.

EXPERIMENTAL

The spectrograms upon which this investigation is based were obtained with the three-meter grazing incidence vacuum spectrograph at the Ohio State University; they cover the range 100–1000Å. A condensed spark between electrodes of columbium or molybdenum wires in carbon and in copper was used to excite the spectra. Different stages of ionization were distinguished by varying the capacity from 0.1 to 1.8 μf , and by varying the inductance in the circuit. Exposures of two to four hours were made on Ilford Q-II plates. Standard wave-lengths in carbon, nitrogen, and oxygen were taken from the table of Boyce and Robinson;² those in copper were taken from the table of Kruger and

Cooper.³ A supplementary spectrogram of the copper spectrum was taken for the purpose of identifying copper lines not published in the table of Kruger and Cooper. It is estimated that the wave-lengths given below are accurate to 0.01Å.

THE SPECTRA OF CB V AND MO VI

Classifications in these spectra isoelectronic with Rb I were given by Trawick;⁴ Table I summarizes the measurements made on the classified lines lying in the range of the present instrument. The lines $4d^2D_{5/2}-4f^2F^{\circ}$ have now been resolved. The agreement between the present measurements and those of Trawick is quite satisfactory except for the multiplet $4d-4f$ in Mo VI; the present measurements place the $4f$ levels about 400 cm^{-1} lower than their position according to Trawick. Attempts to find higher members of the series $4d-np$ and $4d-nf$ by extrapolation of the quantum defects of the np and nf levels proved fruitless except for the transition $4d-6p$ in Mo VI, for which tentative identification is given in Table I.

Table II gives the relative values of the levels in these spectra, measured from $4d^2D_{3/2}$.

* Now at the University of Oklahoma, Norman, Oklahoma.

¹ W. F. Meggers, *J. Opt. Soc. Am.* **36**, 435 (1946).

² J. C. Boyce and H. A. Robinson, *J. Opt. Soc. Am.* **26**, 133 (1936).

³ P. Gerald Kruger and F. S. Cooper, *Phys. Rev.* **44**, 826 (1933).

⁴ M. W. Trawick, *Phys. Rev.* **46**, 63 (1934).

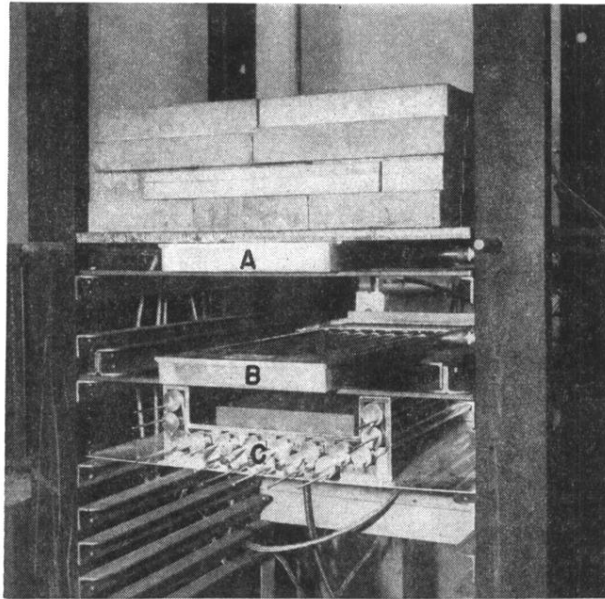


FIG. 2. Photograph of the counter assembly showing the graphite source between trays *B* and *C*. Absorbers are placed in the space between trays *A* and *B*.